Conformational Studies on (17α,20*Z*)-21-(*X*-Phenyl)-19-norpregna-1,3,5(10),20-tetraene-3,17*β*-diols Using 1D and 2D NMR Spectroscopy and GIAO Calculations of ^{13}C Shieldings

Albert B. Sebag, Carolyn J. Friel, Robert N. Hanson,* and David A. Forsyth

Departments of Pharmaceutical Science and Chemistry, Northeastern University, 360 Huntington Avenue, Boston, Massachusetts 02115

r.hanson@nunet.neu.edu

Received May 24, 2000

Differences in agonist responses of the novel estrogen receptor ligands (17α,20*Z*)-(*p*-methoxyphenyl)-vinyl estradiol (**1**), (17α,20*Z*)-(*o*-α,α,α-trifluoromethylphenyl)vinyl estradiol (**2**), and (17α,20*Z*)-(*o*-hydroxymethylphenyl)vinyl estradiol (**3**) led us to investigate their solution conformation. In competitive binding assay studies, we observed that several phenyl-substituted (17α,20*E*/Z)-(*X*-phenyl)vinyl estradiols exhibited significant estrogen receptor binding, but with variation (RBA (**1**) = 20; RBA (**2**) = 23; RBA (**3**) = 140 where estradiol RBA = 100) depending on the phenyl substitution pattern. Because the 17α-phenylvinyl substituent interacts with the key helix-12 of the ligand binding domain, we considered that differences in the preferred conformation of **1**−**3** could account for their varying binding affinity. 2D NMR experiments at 500 MHz allowed the complete assignment of the ^{13}C and ^{1}H spectra of **1**−**3**. The conformations of these compounds in solution were established by 2D and 1D NOESY spectroscopy. A statistical approach of evaluating contributing conformers of **1**−**3** from predicted ^{13}C shifts correlated quite well with the NOE data. The 17α substituents of **1** and **2** exist in similar conformational equilibria with some differences in relative populations of conformers. In contrast, the 17α substituent of **3** exists in a different conformational equilibrium. The similarity in solution conformations of **1** and **2** suggests they occupy a similar receptor volume, consistent with similar RBA values of 20 and 23. Conversely, the different conformational equilibria of **3** may contribute to the significant binding affinity (RBA = 140) of this ligand.

Introduction

Breast cancer is the most common form of cancer among women in the United States, with approximately 181 000 new cases diagnosed annually.[1] It is estimated that one in eight women will develop breast cancer during their lifetime and one in three of those will die from the disease. Among the newly diagnosed cases, about 60% are classified as hormone responsive, defined as containing a minimal level of estrogen receptor (ER) and requiring the presence of circulating estrogen to maintain tumor growth.[2] As part of our program to develop more effective therapeutic agents for the treatment of breast cancer, we undertook the design of new compounds that can potently and selectively block the interaction of estradiol with its target receptor.

Our synthetic efforts have focused on the 17α position of estrogen as the site for introducing substituents that would impart the desired biological properties. Unlike previous studies with 17α alkyl, aryl, or alkynyl groups, suggesting that substituents larger than propyl or propynyl were poorly tolerated,[3] we found that the 17α X-vinyl estradiols could bind quite well to the estrogen receptor.[4] Even large substituents, where X = C_6H_5, SeC_6H_5, or SC_6H_5, exhibited significant relative binding affinities (RBA) for the receptor.[5] These observations led us to pursue the synthesis and evaluation of (17α,20*Z*)-21-(*X*-phenyl)-19-norpregna-1,3,5(10),20-tetraene-3,17*β*-diols (referred to herein as phenylvinyl estradiols) as probes for the estrogen receptor, the results of which are reported in detail elsewhere.[6]

We observed that several phenyl-substituted (17α,20*E*/Z)-(*X*-phenyl)vinyl estradiols exhibited significant estrogen receptor binding (RBA ≥ 20 where estradiol RBA = 100 at 2 °C), but with variation depending on the phenyl substitution pattern (Figure 1). (17α,20*Z*)-(*p*-Methoxyphenyl)vinyl estradiol (**1**), for example, exhibited modest agonist responses in vitro and in vivo and shows an RBA of 20 in vitro, while (17α,20*Z*)-(*o*-α,α,α-trifluoromethylphenyl)vinyl estradiol **2** was similarly potent with an

(1) Greenlee, R. T.; Murray, T.; Bolden, S.; Wingo, P. A. *Cancer J. Clin.* **2000**, *4*, 33.

(2) Iacobelli, S.; King, R. J. B.; Lidner, H. R.; Lippman, M. E. In *Hormones and Cancer*; Raven Press: New York, 1980; Vol. 15, p 337.

(3) (a) Counsell, R. E.; Klimstra, P. D.; Elton, R. L.; Nutting, E. E. *J. Med. Chem.* **1968**, *9*, 689. (b) Raynaud, J. P.; Ojasoo, T. *J. Steroid Biochem.* **1986**, *25*, 811. (c) Salman, M.; Reddy, B. R.; Ray, S.; Stotter, P. L.; Chamness, G. C. *J. Steroid Biochem.* **1988**, *30*, 539.

(4) (a) Hanson, R. N.; El-Wakil, H. *J. Org. Chem.* **1987**, *52*, 3687. (b) Napolitano, E.; Fiaschi, R.; Hanson, R. N. *J. Med. Chem.* **1991**, *34*, 2754. (c) Hanson, R. N.; Napolitano, E.; Fiaschi, R. *J. Med. Chem.* **1998**, *41*, 4686.

(5) (a) Napolitano, E.; Fiaschi, R.; Herman, L. W.; Hanson, R. N. *Steroids* **1996**, *61*, 384. (b) Herman, L. W.; Fiaschi, R.; Napolitano, E. *Steroids* **1996**, *61*, 718. (c) Hanson, R. N.; Napolitano, E.; Fiaschi, R. *Steroids* **1998**, *63*, 479.

(6) (a) Lee, C. Y.; Hanson, R. N., in press. (b) Hanson, R. N.; Lee, C. Y.; Friel, C. *J. Med. Chem.*, submitted for publication. (c) Hanson, R. N.; Friel, C.; Deth, R. C.; DeSombre, E. R.; Metaghee, A. *J. Med. Chem.*, submitted for publication.

10.1021/jo000806h CCC: $19.00
Published on Web 10/13/2000

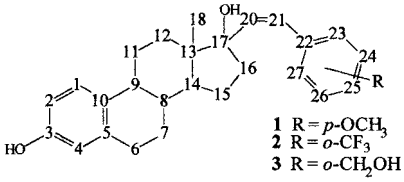

Figure 1. Structures of **1**−**3**.

RBA of 23 in vitro. In stark contrast, (17α,20*Z*)-(*o*-hydroxymethylphenyl)vinyl estradiol (**3**) exhibited significant agonist responses with an RBA of 140, giving **3** more potent estrogen binding affinity than estradiol itself.

Previous studies reveal a considerable interest in the conformation of steroids.[7] These studies indicated that the biological activity of these compounds was related to their conformation. Since the placement of a substituent in the *ortho* or *para* positions could affect the conformation and since the conformational characteristics of 17α-phenylvinyl steroids had not been studied previously, we undertook an investigation of the solution conformation of **1**−**3**. Understanding the preferred conformations is one aspect of an effort to correlate the distinctive biological responses derived from these new probes with their structures and ultimately to associate the responses with the ligand−receptor interactions.

The key conformational feature to establish for **1**−**3** is the positioning of the 17α side chain relative to the steroid skeleton. The conformation of the relatively rigid steroidal skeleton has been established previously by NMR and other methods.[8] In this study, we use molecular mechanics calculations to generate a set of possible conformations. Two types of NMR data are used in conjunction with the predicted conformations to evaluate which conformations are populated in solution. One approach is to use ^{13}C chemical shifts in a comparison with shifts predicted for each of the geometries generated from the molecular mechanics calculations. The predicted ^{13}C shifts come from empirically scaled GIAO (gauge including atomic orbitals) shielding calculations. The other approach is to compare ^{1}H−^{1}H nuclear Overhauser effects established in one- and two-dimensional experiments, 1D and 2D NOESY, with predicted interatomic distances.

NMR Assignments. Before NMR data could be used to evaluate the conformations of **1**−**3**, accurate ^{1}H and ^{13}C chemical shift assignments were required. The one-dimensional ^{1}H spectra of **1**−**3** in acetone-d_6 (Figures 2a, 3a, and 4a) reveal that even at 500 MHz, the low-frequency spectral regions (1.2−2.5 ppm) are unassignable directly as a result of the numerous overlapping signals of the 13 protons resonating in this region. In seeking further separation of the low-frequency region, other deuterated solvents were used, namely, benzene, benzene/acetone, chloroform, chloroform/acetone, and methylene chloride, but pure acetone provides the best separation. Resonances in the low-frequency region that could be readily assigned were the 6α,6β benzylic protons near 2.8 ppm and the C18 methyl ^{1}H signal at 0.9 ppm.[9] Prior literature reports on ^{1}H NMR assignments of estradiol and other steroids are in disagreement and were of little assistance in assigning the remaining low-frequency region.[10] No publication of ^{1}H spectral assignments for any 17α -vinyl-substituted estradiols exists.

The most efficient route to ^{1}H signal assignment was to first assign the ^{13}C spectrum. For **1**−**3**, the ^{13}C experimental shift assignments were based on the study by Dionne and Poirier on ^{13}C assignments of 17α-substituted estradiols and our own DEPT and HMBC experiments.[11] The ^{13}C shift assignments were further supported by theoretical shielding calculations (see below). A heteronuclear multiple quantum coherence (HMQC) experiment was performed to correlate proton signals with directly attached carbons. Because the ^{1}H chemical shift assignments derived from the HMQC experiment depended on the accuracy of the ^{13}C chemical shift assignments, other 2D experiments were performed to provide independent evidence. Homonuclear correlation spectroscopy (H,H-COSY) experiments were performed to correlate the assigned ^{1}H connectivities. The COSY cross-peaks confirmed the initial assignments made by the HMQC experiment. Starting with the unambiguous benzylic H6 signal at 2.8 ppm, the ^{1}H assignments of the entire aliphatic regions of **1**−**3** were confirmed.

The HMQC and H,H-COSY experiments clearly indicated the sites of attachment of all of the protons but did not distinguish between the α and β position of the methylene protons. This distinction was readily achieved by using 2D and 1D nuclear Overhauser effect spectroscopy (NOESY) experiments and by comparing coupling constants. Inspection of the ^{1}H NMR spectrum allows the axial protons, 7α and 6β, to be identified by their larger vicinal coupling constants. The equatorial proton, 11α, is assigned to the isolated signal around 2.4 ppm on the basis of its small coupling constants. The remaining β protons were assigned by the determination of transient NOEs using a 1D NOESY experiment, the 1D analogue of the 2D NOESY experiment.[12] The 1D NOESY experiment avoided problems associated with imperfect subtraction in NOE difference experiments.[13]

Using a selective Gaussian pulse, irradiation of the C18 methyl peaks of **1**−**3** gave signal enhancements for the β-protons at positions 8, 11, 12, 15, and 16 (Figures 2b, 3b, and 4b). These experiments were crucial in making chemical shift assignments, since they resolved β protons from overlapping regions containing α protons. For example, the spectrum of **2** shows a set of four overlapping protons at δ 1.65−1.8 for 12α, 12β, H14 and 15α.

(7) (a) Duax, W. L.; Cody, V.; Grffin, J. F.; Hazel, J.; Weeks, C. M. *J. Steroid Biochem*. **1978**, *9*, 901. (b) Duax, W. L.; Cody, V.; Hazel, J. *Steroids* **1977**, *30*, 471. (c) Duax, W. L.; Weeks, C. M.; Rohrer, D. C.; Osawa, Y.; Wolff, M. E. *J. Steroid Biochem*. **1975**, *6*, 195. (d) Precigoux, G.; Busetta, B.; Courseille, C.; Hospital, M. *Acta Crystallogr., Sect. B* **1975**, *31*, 1527. (e) Kim, R. S.; Labella, F. S.; Zunza, H.; Zunza, F.; Templeton, J. F. *Mol. Pharmacol.* **1980**, *18*, 395.

(8) (a) Marat, K.; Templeton, J. F.; Kumar, V. P. S. *Magn. Reson. Chem*. **1986**, *25*, 25. (b) Barrett, M. W.; Farrant, D. N.; Krik, D. N.; Mersh, J. D.; Sanders, J. K. M.; Duax, W. L. *J. Chem. Soc., Perkin Trans*. **1977**, *30*, 471. (c) Kollman, P. A.; Giannini, D. D.; Duax, W. L.; Rothernberg, S.; Wolff, M. E. *J. Am. Chem. Soc.* **1973**, *95*, 2865. (d) Osawa, Y.; Gardner, J. O. *J. Org. Chem*. **1971**, *36*, 3246.

(9) Kirk, D. N.; Toms, H. C.; Douglas, C.; White, K. A.; Smith, K. E.; Latif, S.; Hubbard, R. W. P. *J. Chem. Soc., Perkins Trans. 2* **1990**, *2*, 10.

(10) (a) Kayser, F.; Biesemans, M.; Pan, H.; Gielen, M.; Willem, R.; Kumar, S.; Schneider, H. J. *J. Chem. Soc., Perkins Trans. 2* **1989**, *2*, 245. (b) Savignac, M.; Jaouen, G.; Rodger, C. A.; Perrier, R. E.; Sayer, B. G.; McGlinchey, M. J. *J. Org. Chem*. **1986**, *51*, 2328. (c) Sedee, A. G.; Henegouwen, M. J. *J. Chem. Soc., Perkins Trans. 2* **1984**, *2*, 1755.

(11) Dionne, P.; Poirier, P. *Steroids* **1995**, *60*, 830.

(12) Kessler, H.; Oschkinat, H.; Griesenger, C.; Bermel, W. *J. Magn. Reson.* **1986**, *70*, 106−133.

(13) Toffanin, R.; Matulova, M.; Bella, J.; Lamba, D.; Cescutti, P.; Paoletti, S.; Kvam, B. J. *Carbohydr. Res.* **1994**, *265*, 151.

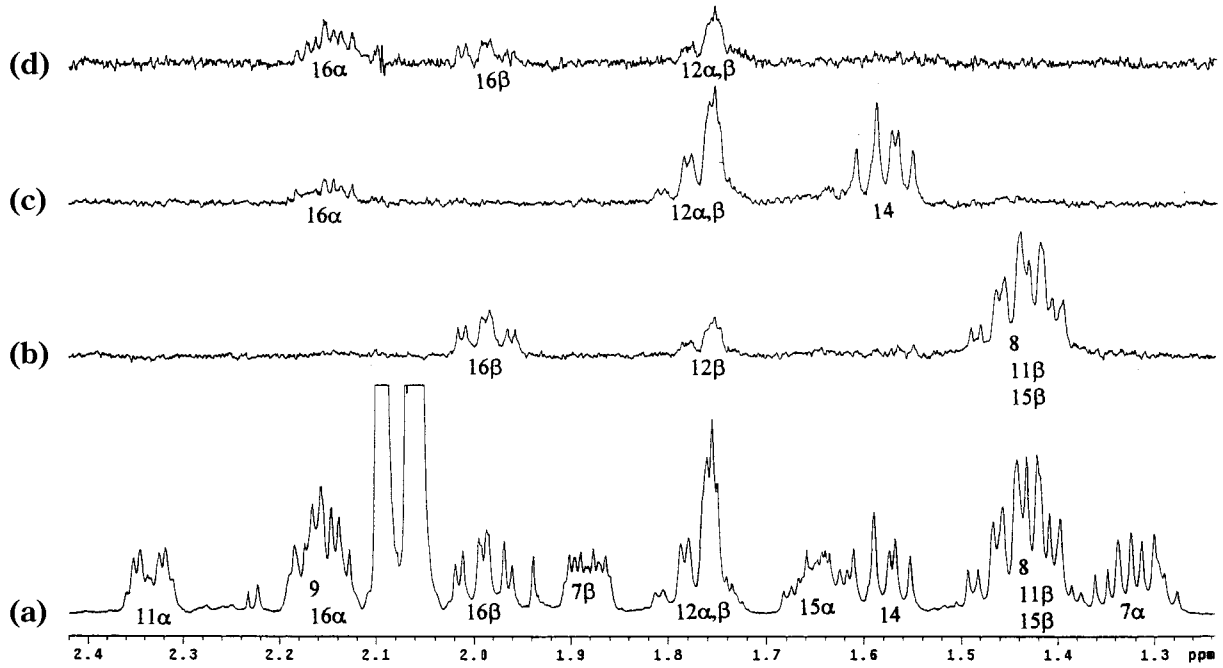

Figure 2. (a) Low-frequency spectral region of the 500 MHz ^{1}H NMR spectra of **1** in acetone-d_6. Equivalent spectral regions of the 500 MHz 1D NOESY spectra (500 ms mixing time) of **1** obtained by selective irradiation of the C18 methyl (b), H20 (c), and H23/27 (d) using a Gaussian pulse. Spectra b and c are 5× the vertical scale of a. Spectra d is 10× the vertical scale of a.

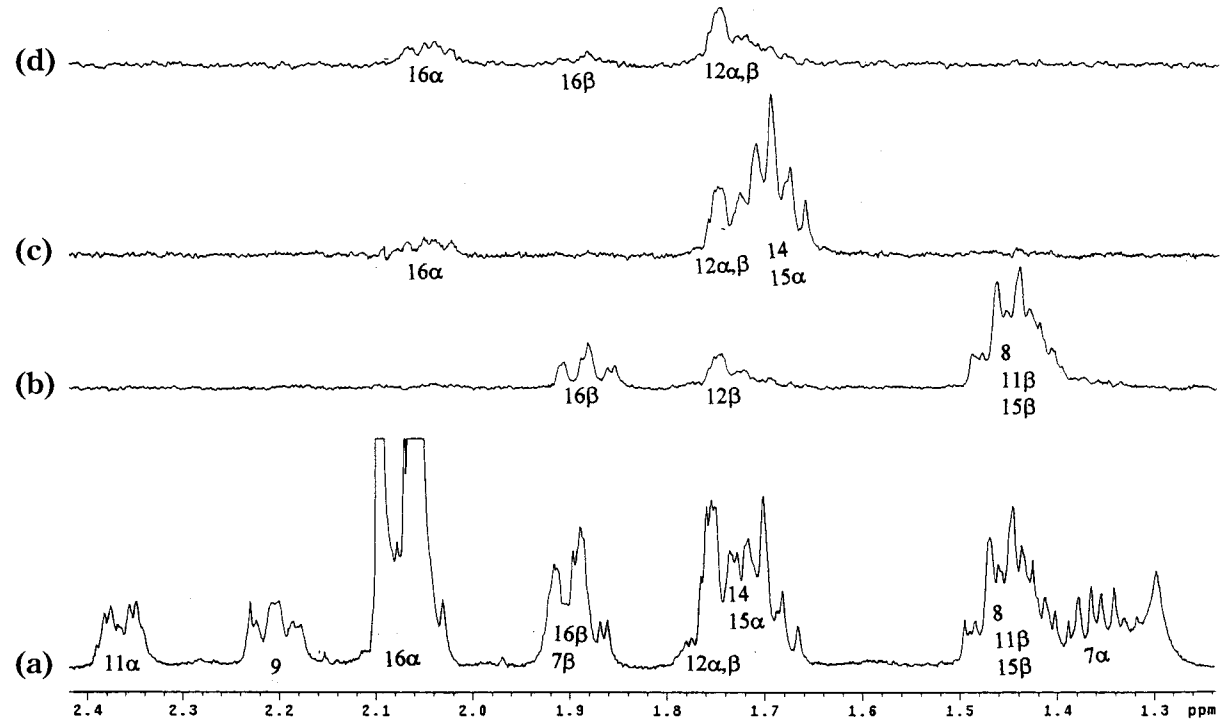

Figure 3. (a) Low-frequency spectral region of the 500 MHz ^{1}H NMR spectra of **2** in acetone-d_6. Equivalent spectral regions of the 500 MHz 1D NOESY spectra (500 ms mixing time) of **2** obtained by selective irradiation of the C18 methyl (b), H20 (c), and H27 (d) using a Gaussian pulse. Spectra b and c are 5× the vertical scale of a. Spectra d is 10× the vertical scale of a.

Irradiation of the C18 methyl, in the 1D NOESY experiment, reveals at 1.75 ppm the expected 12β signal from the overlapping region. The remaining assignments in this set are based on the HMQC of steroid **2** that shows that the H14 and 15α protons are slightly further upfield (1.7 and 1.72 ppm) than 12α or 12β. The remaining signal at 1.77 ppm can therefore be assigned to 12α. Assignments in the B and C ring were validated by other 1D NOESY experiments, including the irradiation of H1 that results in the expected enhancement of 11α and the irradiation of H6, yielding the expected 7α, 7β, and H8 enhancements. In summary, consideration of all the independent NMR experiments allowed the unambiguous assignment of all ^{1}H and ^{13}C resonances. Table 1 summarizes all of the ^{1}H and ^{13}C chemical shifts for **1**−**3**.

Theoretical Carbon Chemical Shifts and Solution Conformations. The predicted low-energy conformers of **1**−**3** were generated using the MM3 force field and

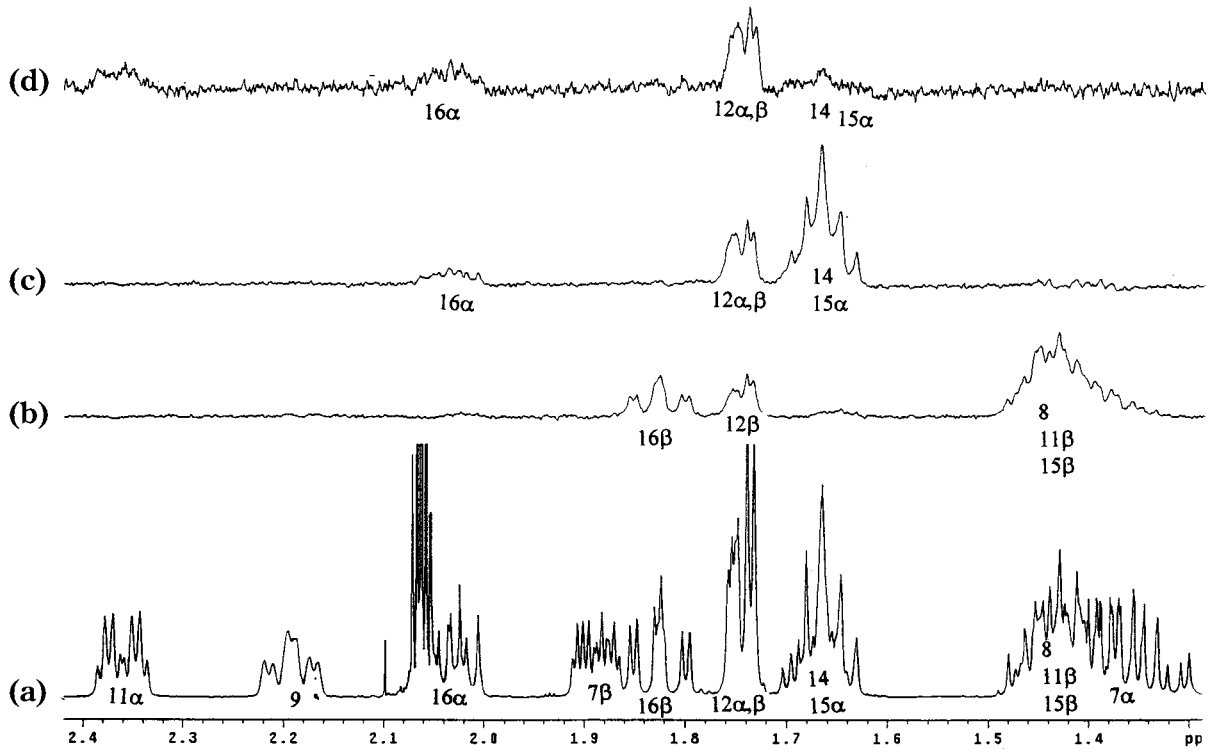

Figure 4. (a) Low-frequency spectral region of the 500 MHz ^{1}H NMR spectra of **3** in acetone-d_6. Equivalent spectral regions of the 500 MHz 1D NOESY spectra (500 ms mixing time) of **3** obtained by selective irradiation of the C18 methyl (b), H20 (c), and H23/27 (d) using a Gaussian pulse. Spectra b and c are 5× the vertical scale of a. Spectra d is 15× the vertical scale of a.

Table 1. ^{1}H and ^{13}C Chemical Shifts for 1−3

^{1}H	**1**	**2**	**3**	^{13}C	**1**	**2**	**3**
1	7.12	7.12	7.12	1	126.9	127.4	126.5
2	6.60	6.62	6.62	2	113.5	113.9	113.2
4	6.54	6.60	6.58	3	155.8	155.0	153.2
6α	2.75	2.78	2.79	4	115.8	116.2	115.2
6*β*	2.80	2.81	2.82	5	138.3	139.1	137.5
7α	1.32	1.38	1.34	6	29.9	30.7	29.8
7*β*	1.88	1.88	1.88	7	28.5	28.7	27.9
8	1.43	1.48	1.43	8	40.7	41.2	40.2
9	2.18	2.20	2.18	9	44.5	45.0	44.0
11α	2.33	2.38	2.36	10	131.9	131.9	131.9
11*β*	1.46	1.45	1.46	11	27.3	27.7	26.8
12α	1.77	1.77	1.76	12	32.6	33.7	33.0
12*β*	1.75	1.75	1.74	13	48.7	49.0	48.0
14	1.57	1.70	1.66	14	49.9	50.8	49.9
15α	1.64	1.72	1.68	15	23.7	24.4	23.4
15*β*	1.41	1.43	1.40	16	38.3	39.3	38.4
16α	2.16	2.06	2.02	17	83.8	85.8	84.8
16*β*	1.98	1.90	1.82	18	14.5	14.8	14.6
CH_3	0.96	0.90	0.88	20	135.1	138.7	138.0
20	5.88	6.10	6.03	21	129.7	124.2	125.0
21	6.39	6.59	6.50	22	130.5	137.8	138.2
23	7.63	N/A	N/A	23	132.4	133.3	138.5
24	6.86	7.61	7.36	24	113.6	125.9	129.0
25	N/A	7.52	7.20	25	159.4	131.9	126.8
26	6.86	7.39	7.18	26	113.6	130.5	127.8
27	7.63	7.64	7.21	27	132.4	132.3	126.8
28[a]	3.80	N/A	4.60	28[a]	55.3	127.6	62.5

[a] Additional alkyl: 1, OCH_3; 2, CF_3; 3, CH_2OH.

were initially determined by rotation around dihedrals C13−C17−C20−C21 and C20−C21−C22−C23 (Figures 5−7).[14] The OH and OCH_3 groups were then rotated so as to find the lowest energy position. For **3**, hydrogen bonding between the 17-OH and 23-CH_2OH group resulted in three pairs (**3a**/**3c**, **3b**/**3d**, **3e**/**3f**) of proton donor/acceptor conformers. The key dihedral angles for the lowest energy conformers, **1a**−**e**, **2a**−**f**, and **3a**−**h**, with energies within 6 kcal of the lowest energy conformer for **1**−**3**, are listed in Table 2. Conformers **1d**, **2d**, **3e**, and **3f**, which have an orthogonal alignment between the estradiol skeleton and the 17α substituent and an anti alignment between the phenyl ring and the C18 methyl, are referred to herein as anti orthogonal conformers. Conversely, conformers **1a**, **2a**, **3a**, and **3c** will be referred to as syn orthogonal conformers. Conformers **1b**, **2b**, **2c**, **3b**, **3d**, and **3h** are designated as extended conformers. All other conformers will be described via a combination of these names.

As the MM3 calculations show, significant changes in the 17α side chain conformation result in minor energy differences. In fact, most of the low-energy conformers are within 3 kcal of the lowest energy conformer. This made any conformational determination based purely on energy predictions unreliable.

More reliable conclusions regarding the 17α side chain conformation of **1**−**3** could be achieved by comparing predicted ^{13}C chemical shifts for each MM3 conformer to experimental shifts. These predicted ^{13}C chemical shifts, δ_{pred}, were calculated by empirically scaling GIAO-calculated absolute shieldings, σ.[15] The appropriate scaling equation depends on the basis set. In this study, in which GIAO shielding calculations were obtained at the B3LYP/3-21G level with heteroatoms augmented at the 6-31+G* level, the appropriate scaling is given by eq 1,

$$\delta_{pred} = -1.168\sigma + 230.2 \qquad (1)$$

(14) (a) Allinger, N. L.; Yuh, Y. H.; Lii, J. H. *J. Am. Chem. Soc.* **1989**, *111*, 8551, 8566, 8576. (b) *MM3(94)*; Tripos, Inc.: St. Louis, MO.

(15) (a) Ditchfield, R. *Mol. Phys.* **1974**, *27*, 789. (b) Rohling, C. M.; Allen, L. C.; Ditchfield, R. *Chem. Phys.* **1984**, *87*, 9. (c) Wolinski, K.; Hinton, J. F.; Pulay, P. *J. Am. Chem. Soc.* **1990**, *112*, 8251.

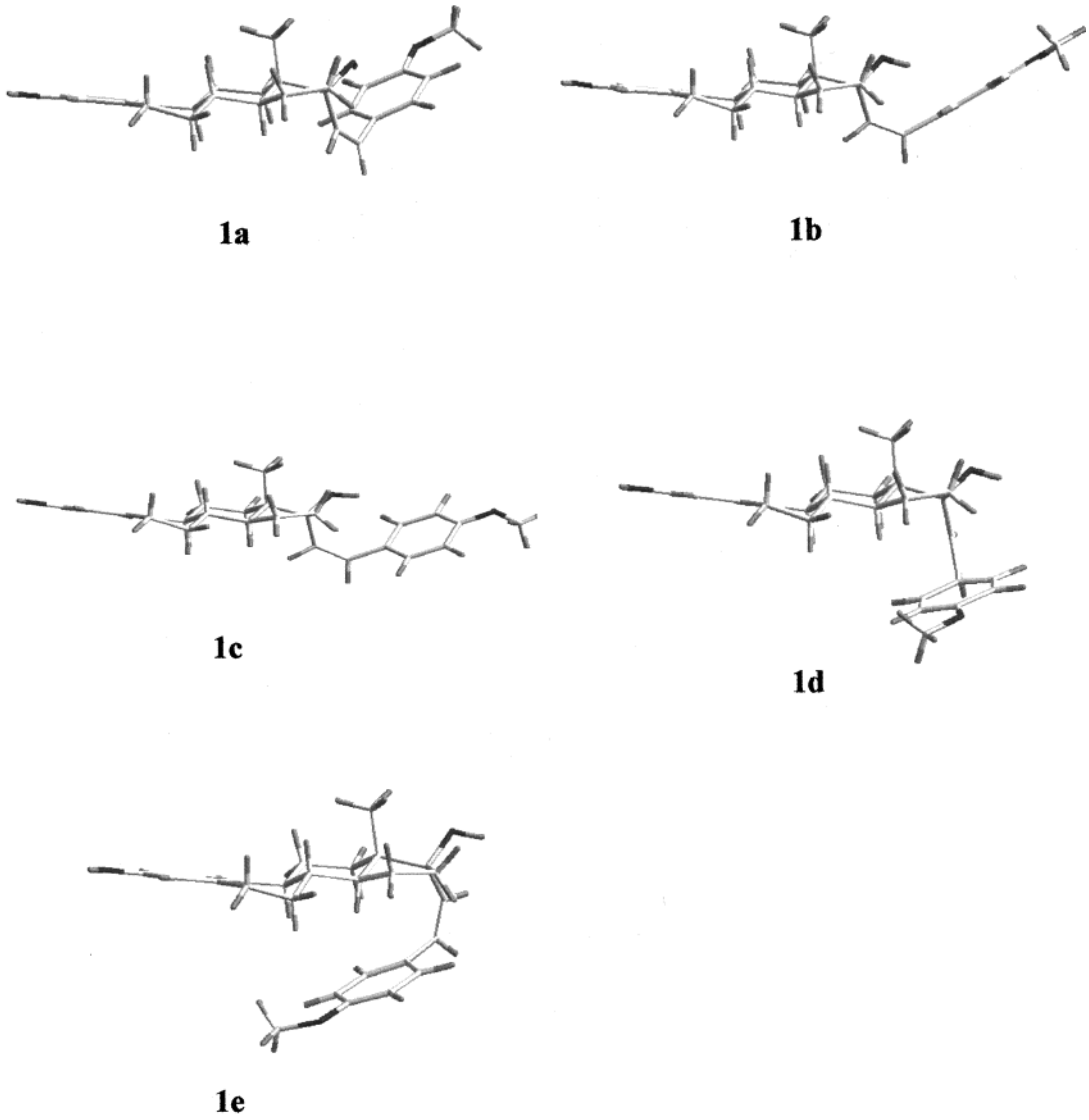

Figure 5. MM3-predicted geometries for the most stable conformers of **1**.

as determined previously.[16]All calculations were carried out with the Gaussian 98 program.[17] Tables 3−5 list the predicted ^{13}C chemical shifts of each MM3 conformer and the assigned experimental ^{13}C chemical shifts for **1**−**3**.

Previously, Dionne and Poirier showed that the carbons in the A, B, and C ring experience little shielding or deshielding effects from various 17α substituents since these carbons exhibit minor (∼1 ppm) chemical shift changes. However, carbons in the D ring were significantly influenced by various 17α substituents. Specifically, C16 and C17 were shown to be the most heavily influenced. Our predicted ^{13}C chemical shifts correspond quite well with the carbons in rings A, B, and C (C1−C14); in fact, most of the ^{13}C predictions in rings A, B, and C are within 1 ppm of the assigned experimental values. These results demonstrate the accuracy of these predictions in an area of a well-defined geometry without any conformational distinction. The shielding and deshielding effects of the 17α substituent are clearly evident in the predicted chemical shift of C16 in different conformers of **1**. In conformers **1b** and **1e**, respectively the second lowest and the highest energy conformers of **1**, the predicted shifts of C16 differ by more than 8 ppm from the experimental value. Similarly for **2** and **3**, the predicted ^{13}C chemical shifts of C16 differ from the observed shift by more than 4 ppm for conformer **2d** and 5 ppm for conformers **2b**, **3f**, and **3h**. These large differences of the predicted shifts of C16 among similar conformers are attributed to the steric interactions between the ortho protons H23/27 and 16α. For example, the predicted C16 shift for extended conformer **1b** with a spatial distance between H23/27 and 16α of 2.2 D differs from experiment by more than 8 ppm, while the C16 shift prediction for anti orthogonal/extended conformer **1c** with a distance between H23/27 and 16α of 3.2 D is within 1 ppm of the experimental value.

(16) Forsyth, D. A.; Sebag, A. B. *J. Am. Chem. Soc.* **1997**, *119*, 9483.
(17) *Gaussian 98*, Revision A.3; Frisch, M. J.; Trucks, G. W.; Schlegel, H. B.; Scuseria, G. E.; Robb, M. A.; Cheeseman, J. R.; Zakrzewski, V. G.; Montgomery, J. A., Jr.; Stratmann, R. E.; Burant, J. C.; Dapprich, S.; Millam, J. M.; Daniels, A. D.; Kudin, K. N.; Strain, M. C.; Farkas, O.; Tomasi, J.; Barone, V.; Cossi, M.; Cammi, R.; Mennucci, B.; Pomelli, C.; Adamo, C.; Clifford, S.; Ochterski, J.; Petersson, G. A.; Ayala, P. Y.; Cui, Q.; Morokuma, K.; Malick, D. K.; Rabuck, A. D.; Raghavachari, K.; Foresman, J. B.; Cioslowski, J.; Ortiz, J. V.; Stefanov, B. B.; Liu, G.; Liashenko, A.; Piskorz, P.; Komaromi, I.; Gomperts, R.; Martin, R. L.; Fox, D. J.; Keith, T.; Al-Laham, M. A.; Peng, C. Y.; Nanayakkara, A.; Gonzalez, C.; Challacombe, M.; Gill, P. M. W.; Johnson, B.; Chen, W.; Wong, M. W.; Andres, J. L.; Gonzalez, C.; Head-Gordon, M.; Replogle, E. S.; Pople, J. A. Gaussian, Inc., Pittsburgh, PA, 1998.

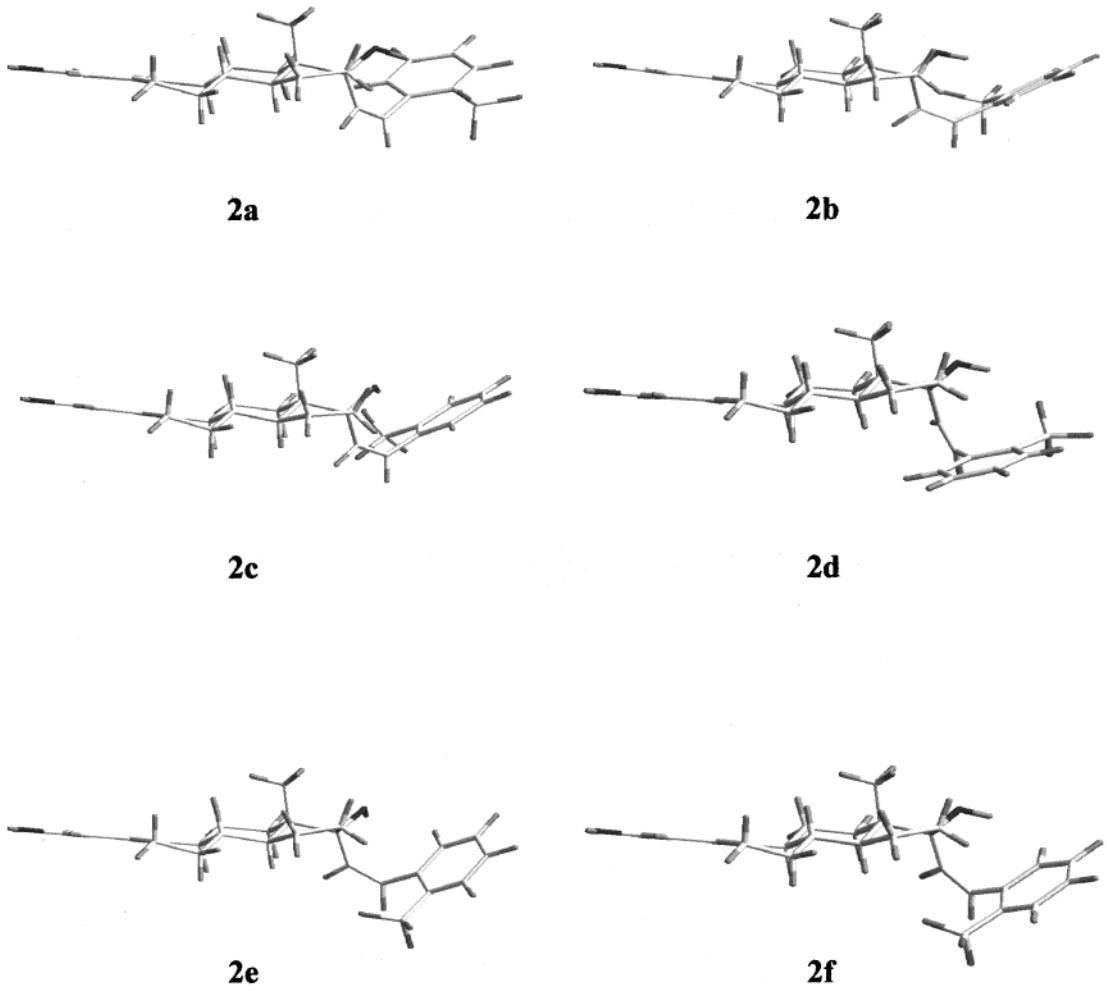

Figure 6. MM3-predicted geometries for the most stable conformers of **2**.

If **1**−**3** are rapidly exchanging among conformers, only average positions of the ^{13}C resonances will be observed experimentally on the NMR time scale. To determine the contributing conformers of **1**−**3,** we chose a statistical approach in which the predicted ^{13}C shifts of the C and D rings of all reasonable conformers of **1**−**3** were in each separate case treated as independent variables in a multiple independent variable regression analysis of the corresponding experimental data.[18] The predicted ^{13}C shifts of the A and B rings of all reasonable conformers of **1**−**3** were not used in this statistical analysis since they are all within 1 ppm of the experimental values regardless of the conformer. The regression analysis yielded fractional populations as the fitting parameters. All standard errors and confidence levels of the regression analysis were estimated using the Bootstrapping method.[19] The results and corresponding estimates of uncertainties (standard errors) are listed in Table 6. Both **1** and **2** were found to have a major conformer, **1c** 68(24)% and **2c** 60-(1)%. Two minor conformers are also indicated for each: **1a** 20(12)% and **1d** 12(30)%, and **2a** 20(13)% and **2f** 20-(8)%. For **3**, conformers **3a** 36(14)%, **3d** 34(26)%, and **3e** 28(14)% were found to be similarly populated. It is important to note that the large corresponding standard error of certain contributing conformers renders conclusions on their presence unreliable. This is evident with predicted conformer **1d** that is estimated to be 12% present but has a 30% standard error.

NOESY Studies. The solution state conformations of the 17α side chain of **1**−**3** were also probed by 2D and 1D NOESY experiments. In the case of **1**, the low-frequency region of the 2D NOESY spectrum reveals strong cross-peaks involving the vinyl proton, H20, with H14 and 12α,*β*. A weaker cross-peak with 16α could also be detected. The 2D NOESY spectrum also reveals weak cross-peaks between the H23/27 aryl protons and four alkyl protons, 12α, 12*β*, 16α, and 16*β*. The NOE data provide evidence for more than one conformer since no single conformer of **1** is expected to have an NOE with either H23 or H27 and both 12α and 16α. As all of the predicted low-energy conformers of **1** show, structures with a distance between H23 or H27 and 12α appropriate for an NOE preclude an NOE with 16α as a result of too great of a distance (>5 Å). Conformer **1c**, for example, which has a distance between H27 and 16α of 3.2 Å, has a distance greater than 5 Å between H23 or H27 and 12α.

In keeping with the 2D NOESY results for **1**, the selective 1D NOESY of H20 reveals equally strong enhancements of 12α,*β* and H14 and a weak enhancement of 16α (Figure 2c). Similarly, the 1D NOESY of H23/27 shows weak enhancement of 12α, 12*β*, 16α, and 16*β* (Figure 2d). Comparison of the intensity of these enhancements suggests a similarly short distance be-

(18) *SPSS*, V. 10, SPSS Inc.: Chicago, IL.
(19) Mooney C. Z.; Duval R. D. *Bootstrapping*; Sage Publications: Newbury Park, CA, 1993.

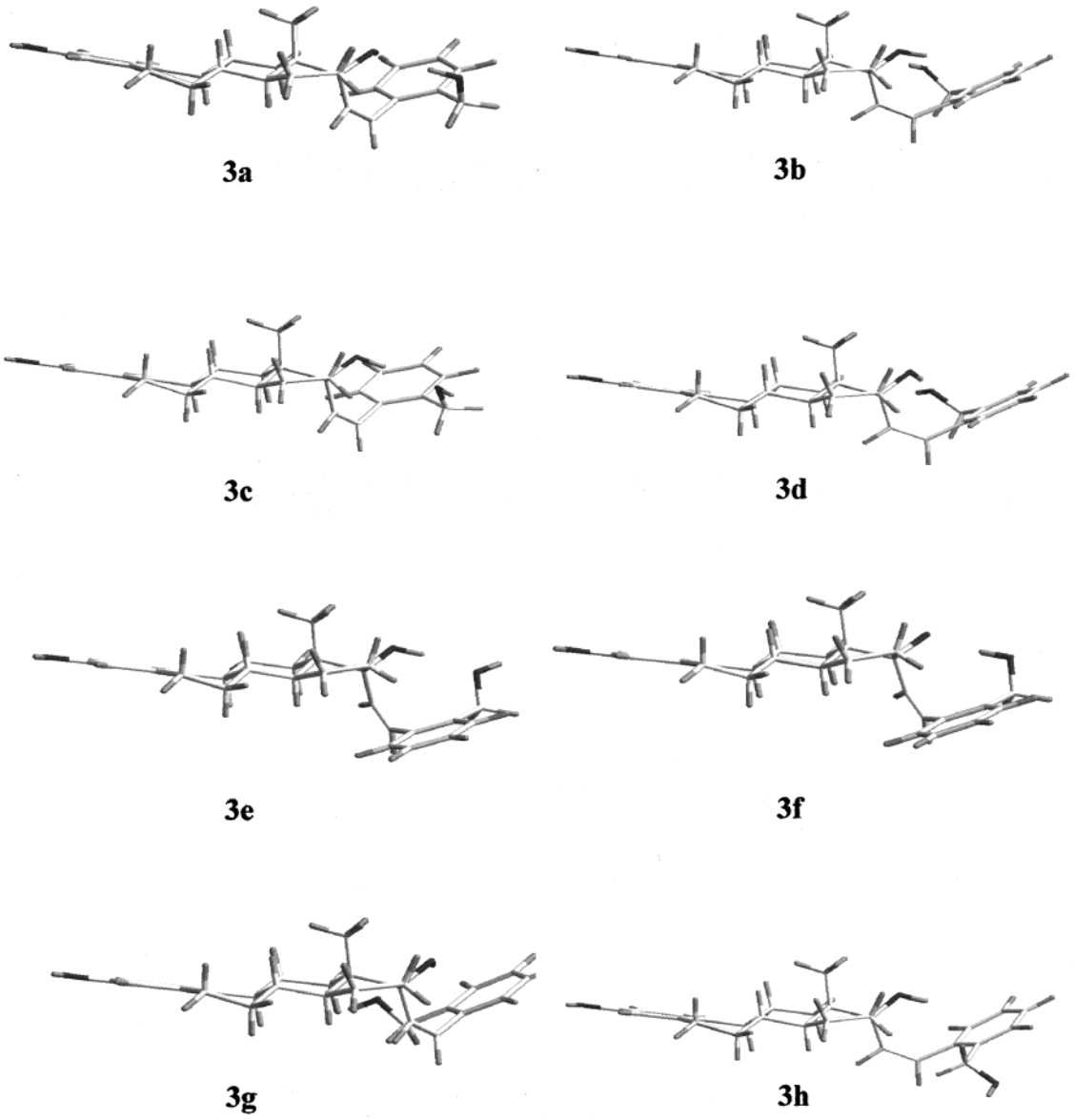

Figure 7. MM3-predicted geometries for the most stable conformers of **3**.

Table 2. Relative Energies and Key Dihedrals of Predicted Conformers of 1−3 Using MM3

conformers	C13−C17−C20−C21	C20−21−22−23	rel energies (kcal/mol)
1a	−103	−86	0
1b	−156	−68	0.6
1c	−110	−110	3
1d	105	86	3.2
1e	70	81	5.7
2a	−112	−99	0
2b	−151	109	0.3
2c	−148	93	1.7
2d	118	85	2.1
2e	162	−125	2.3
2f	145	−118	3.1
3a	106	90	0
3b	155	98	0.6
3c	109	94	2.3
3d	150	78	2.6
3e	−131	−81	3.3
3f	−132	−81	3.7
3g	111	105	4.2
3h	153	89	4.9

tween H20 and 12α,*β* and between H20 and H14, as well as greater distances between H20 and 16α and between H23/27 and 12α, 12*β*, 16α, and 16*β*. Table 7 summarizes and compares the intensity of the observed NOE signals with expected NOEs based on H−H distances in all predicted low-energy conformers of **1**. Comparison of these observed enhancements with expected NOE intensities for all predicted low-energy conformers of **1** rules out conformers **1d** and **1e** as contributing conformers based on the absence of observable NOE signals involving H23/27 with H14 and 15α. The strong, equally enhanced NOE signals between H20 and 12α and between H20 and H14 suggest that the major conformer bears an extended side chain geometry, consistent with conformers **1b** and **1c**. In comparing conformers **1b** and **1c**, the weak NOE signal between H23/27 and 16α is consistent with the expected weak NOE intensity between H23/27 and 16α of conformer **1c** and inconsistent with the expected strong NOE intensity between H27 and 16α of conformer **1b**. Therefore, conformer **1c** is considered the major conformer.

The weak NOE signal between H23/27 and 12α,*β*, which is not expected to arise from conformers **1b** or **1c** since these conformers have distances greater than 5 Å

Table 3. Experimental and Predicted ^{13}C Chemical Shifts (ppm) of Predicted Conformers of 1 Using B3LYP/3-21G(X,6-31+G*)//MM3 Calculations

	1a	1b	1c	1d	1e	expt
C1	127.5	127.6	127.5	127.5	127.4	126.9
C2	113.0	113.0	113.1	113.0	112.8	113.5
C3	152.9	152.9	153.0	152.9	152.6	155.8
C4	115.6	115.6	115.7	115.6	115.7	115.8
C5	136.3	136.2	136.1	136.1	136.1	138.3
C6	31.0	31.1	31.1	31.0	30.7	29.9
C7	28.4	28.4	28.4	28.5	27.0	28.5
C8	40.1	39.8	39.7	39.6	38.7	40.7
C9	44.3	44.4	44.3	44.3	42.5	44.5
C10	132.1	132.1	132.2	132.3	132.3	131.9
C11	28.5	28.4	28.5	28.5	28.5	27.3
C12	34.2	32.0	31.9	32.8	34.0	32.6
C13	48.6	48.0	47.6	48.4	49.8	48.7
C14	50.7	48.7	49.1	49.0	47.3	49.9
C15	26.0	26.8	26.1	25.3	27.1	23.7
C16	39.8	46.6	38.1	37.5	46.6	38.3
C17	86.1	83.4	79.7	83.0	86.1	83.8
C18	16.0	15.3	14.3	15.1	16.1	14.5
C20	142.2	144.5	142.4	142.9	152.0	135.1
C21	133.1	130.8	134.8	135.3	134.5	129.7
C22	127.8	129.6	130.4	129.5	132.1	130.5
C23	129.2	130.1	127.4	131.7	129.1	132.4
C24	117.1	118.8	119.2	117.1	118.7	113.6
C25	157.5	157.5	157.6	156.9	157.4	159.4
C26	109.4	110.0	110.8	109.2	110.1	113.6
C27	132.2	128.6	128.8	129.6	130.9	132.4
C28	54.0	54.0	54.6	54.0	54.5	55.3

Table 4. Experimental and Predicted ^{13}C Chemical Shifts (ppm) of Predicted Conformers of 2 Using B3LYP/3-21G(X,6-31+G*)//MM3 Calculations

	2a	2b	2c	2d	2e	2f	expt
C1	127.3	127.6	127.6	127.5	127.6	127.4	127.4
C2	113.0	113.1	113.1	113.0	113.0	113.0	113.9
C3	153.0	153.0	152.9	153.0	152.9	153.2	155.0
C4	115.9	115.8	115.6	115.7	115.8	115.7	116.2
C5	136.0	136.0	135.9	136.1	136.3	136.3	139.1
C6	30.9	31.0	30.9	31.1	31.1	31.1	30.7
C7	28.3	28.4	28.4	28.4	28.1	28.0	28.7
C8	39.7	39.7	40.0	39.8	39.9	40.1	41.2
C9	44.1	44.0	44.4	44.1	43.9	44.0	45.0
C10	131.9	132.1	132.1	132.0	131.9	132.0	131.9
C11	28.5	28.4	28.3	28.6	28.4	28.6	27.7
C12	34.9	32.1	33.9	32.3	30.8	30.9	33.7
C13	48.0	47.9	49.3	48.0	47.7	48.0	49.0
C14	50.1	49.5	50.5	49.1	49.1	48.7	50.8
C15	26.5	26.8	26.3	26.3	25.8	26.1	24.4
C16	42.6	45.1	39.3	35.0	40.6	36.1	39.3
C17	86.1	84.4	87.8	81.8	81.8	80.5	85.8
C18	14.6	15.1	16.1	14.7	15.4	15.0	14.8
C20	143.7	147.0	141.6	142.0	145.5	140.6	138.7
C21	127.8	126.2	129.2	129.4	132.0	133.3	124.2
C22	138.9	138.9	135.5	139.8	139.2	140.5	137.8
C23	129.2	133.4	131.5	132.4	131.1	130.5	133.3
C24	125.9	127.2	127.4	126.6	129.2	128.1	125.9
C25	130.7	128.8	131.1	130.6	130.8	130.4	131.9
C26	131.7	131.0	130.2	131.4	132.0	131.7	130.5
C27	132.2	128.8	134.5	129.4	129.6	130.8	132.3
C28	127.0	127.1	127.4	126.7	127.3	127.0	127.6

between H23/27 and 12α,*β*, supports the presence of the syn orthogonal conformer **1a**.

In regard to conformations for **2**, the low-frequency region of the 2D NOESY spectrum of **2** displays a strong cross-peak between H20 and an overlapping region consisting of 12α, 12*β*, H14, and 15α. Additionally, weak cross-peaks between H27 and 12α,*β*, 16α, and 16*β* are observable. This pattern of NOESY cross-peaks is similar to that observed for **1**. An additional weak cross-peak between H21 and 12α,*β* could also be detected. A selective 1D NOESY of H20 reveals that the strong cross-peak

Table 5. Experimental and Predicted ^{13}C Chemical Shifts (ppm) of Predicted Conformers of 3 Using B3LYP/3-21G(X,6-31+G*)//MM3 Calculations

	3a	3b	3c	3d	3e	3f	3g	3h	expt
C1	127.4	127.6	127.4	127.4	127.5	127.3	127.3	127.3	126.5
C2	113.1	113.2	112.9	112.9	112.8	113.0	112.9	113.0	113.2
C3	153.1	153.0	152.8	152.9	152.8	153.1	152.9	152.9	153.2
C4	115.9	115.7	115.7	115.7	115.6	115.8	115.7	115.8	115.2
C5	136.0	136.0	136.1	136.3	136.3	136.3	136.1	136.1	137.5
C6	30.9	31.0	31.0	31.1	31.2	31.0	31.1	31.0	29.8
C7	28.2	28.5	28.4	28.5	28.3	28.1	28.5	28.4	27.9
C8	39.8	39.7	39.6	40.0	40.0	40.1	40.1	39.6	40.2
C9	44.0	44.1	44.2	44.4	44.0	43.8	44.5	44.3	44.0
C10	131.7	131.8	132.5	132.3	132.4	131.4	132.2	132.1	131.9
C11	28.4	28.3	28.6	28.5	28.7	28.4	28.6	28.5	26.8
C12	34.3	31.3	34.9	31.9	31.7	30.4	33.0	32.3	33.0
C13	48.0	47.5	47.8	48.0	47.7	48.1	49.1	48.3	48.0
C14	50.4	49.2	50.1	49.2	49.3	49.1	50.8	49.3	49.9
C15	26.2	26.6	26.8	26.1	25.7	25.0	26.2	26.7	23.4
C16	39.4	44.9	43.3	42.0	34.4	30.9	39.2	43.6	38.4
C17	85.9	83.3	85.4	84.4	79.9	80.2	87.3	85.8	84.8
C18	16.1	15.3	14.7	16.0	15.5	15.4	16.0	14.9	14.6
C20	141.6	144.6	145.0	146.1	142.8	136.2	141.7	141.5	138.0
C21	130.9	129.6	128.3	127.8	129.2	136.5	130.5	127.8	125.0
C22	134.5	136.4	140.2	140.6	140.5	135.5	133.4	134.3	138.2
C23	141.0	140.6	133.2	133.5	135.9	140.4	136.4	140.0	138.5
C24	131.9	131.7	131.4	131.2	132.5	131.8	130.0	130.4	129.0
C25	128.5	126.8	128.5	126.9	126.9	127.9	127.7	127.9	126.8
C26	126.0	128.3	127.0	128.8	128.3	126.2	126.2	126.6	127.8
C27	131.9	131.7	131.4	131.2	127.7	131.8	132.8	126.5	126.8
C28	64.5	65.0	65.9	66.2	64.7	64.1	63.2	63.3	62.5

Table 6. Summary of the Multiple Independent Variable Regression Analysis[a] of the Calculated ^{13}C Shifts of Predicted Conformers of 1−3

conformer	estimate (%)	standard error (%)
1a	20	12
1b	0	7
1c	68	24
1d	12	30
1e	0	0
2a	20	13
2b	0	15
2c	60	1
2d	0	7
2e	0	11
2f	20	8
3a	36	14
3b	0	1
3c	0	5
3d	34	26
3e	28	14
3f	0	1
3g	2	7
3h	0	10

[a] Constraints: Each conformer is greater than or equal to 0%. Conformer sets **1a**−**e**, **2a**−**f**, and **3a**−**h** are equal to 100%.

consists mainly of signal from H14 with some contribution from 12α,*β* (Figure 3c). The 1D NOESY of H20 also displays a very weak enhancement of 16α. The 1D NOESY of H27 displays the expected weak enhancements of 12α,*β*, 16α, and 16*β* expected from the 2D NOESY experiment (Figure 3d). The NOE data indicates the presence of at least two conformers with rotated phenyl rings since no predicted conformer of **2** is expected to have an NOE with H27 and both 12α and 16*β*.

As described in detail below, comparing these observed enhancements with expected NOE intensities for predicted conformers of **2** suggests that conformer **2c** is the major conformer with minor contribution from **2a** and other conformers as well (see Table 8).

Table 7. Summary and Comparison of Observed NOE Enhancements with Expected NOE Intensities[a] for Predicted Conformers of 1

irradiated	enhanced	**1a**	**1b**	**1c**	**1d**	**1e**	expt
H20	12α,*β*	w	s	s	s	w	s
H20	H14	s	s	s	w	w	s
H20	16α	s	w	w	w	w	w
H23/27	12α,*β*	s	n	n	w	s	w
H23/27	H14	n	n	n	s	s	n
H23/27	15α	n	n	n	w	s	n
H23/27	16α	n	s	w	s	s	w
H23/27	16*β*	n	w	w	w	s	w

[a] Expectations of strong (s), weak (w), and no (n) NOE enhancements correspond to H−H distances of 0−2.99, 3.0−4.99, and >5 Å.

Table 8. Summary and Comparison of Observed NOE Enhancements with Expected NOE Intensities[a] for Predicted Conformers of 2

irradiated	enhanced	**2a**	**2b**	**2c**	**2d**	**2e**	**2f**	expt
H20	12α,*β*	w	s	s	s	s	s	s
H20	H14	s	s	s	w	s	w	s
H20	16α	s	w	w	w	w	w	w
H21	12α,*β*	w	n	n	n	n	n	w
H27	12α,*β*	s	n	n	w	n	n	w
H27	H14	n	n	n	s	n	n	n
H27	15α	n	n	n	s	n	n	n
H27	16α	n	s	w	w	n	s	w
H27	16*β*	n	w	w	n	w	w	w

[a] Expectations of strong (s), weak (w), and no (n) NOE enhancements correspond to H−H distances of 0−2.99, 3.0−4.99, and >5 Å.

The observed strong and moderately strong enhancements of H14 and 12α,*β*, respectively, upon irradiation of H20 suggests that the 17α side chain of the major conformer bears an extended geometry with a closer distance between H20 and H14 than between H20 and 12α,*β*. This is only consistent with conformers **2b** and **2c**, which have distances between H20 and H14 of 2.0 and 2.2 Å and between H20 and 12α of 2.1 and 2.5 Å, respectively. Comparing **2b** and **2c**, the weak enhancement of 16α upon irradiation of H27 is consistent with the expected weak NOE intensity between H27 and 16α of conformer **2c** but is inconsistent with the expected strong NOE intensity between H27 and 16α of conformer **2b**. Conformer **2c** thus is considered the major conformer.

As for minor conformers, conformer **2d** can be ruled out as a contributing conformer because of the absence of an observable NOE between H27 and H14 or 15α. For conformer **2f**, the expected weak enhancement of H14 upon irradiation of H20 suggests only a minor contribution since the observed enhancement is strong. The geometrically similar conformer, conformer **2e**, could not be ruled out with NOE data as a minor conformer. The presence of the syn orthogonal conformer **2a** is clear from the NOE enhancement of 12α,*β* upon irradiation of H27. All other conformers of **2** have a distance between H27 and 12α,*β* greater than 5 Å. The NOESY cross-peak between H21 and 12α,*β* further supports the presence of conformer **2a** since all other predicted conformers bear a distance between H21 and 12α,*β* greater than 5 Å.

The low-frequency region of the 2D NOESY spectrum of **3** displays additional cross-peaks not found in the similarly patterned 2D NOESY of **1** and **2** (Figure 8). Aside from the cross-peaks between H20 with 12α,*β*, H14, and 16α and H27 with 12α,*β* and 16α analogous to those observed for **1** and **2**, additional weak cross-peaks between H21 and H27 with an overlapping region consisting of H14 and 15α appear. Also, weak cross-peaks between the methylene protons of the 23-CH_2OH group and 12α,*β* and 16α are observable. A selective 1D NOESY of H20 reveals strong enhancements of H14 and 12α,*β* and weak enhancement of 16α (Figure 4c). The 1D NOESY of H27 displays the expected weak enhancements of 16α and the overlapped regions consisting of 12α,*β* and H14,15α (Figure 4d).

Comparing these observed enhancements with expected NOE intensities for predicted conformers of **3** indicates the presence of at least three conformers (see Table 9). The observed weak NOE enhancements of H21 with H14 and H27 with the overlapped region consisting of H14 and 15α are only consistent with the two predicted anti orthogonal conformers **3e** and **3f**. All other conformers of **3** have a distance between these protons greater than 5 Å. Similarly, the observed weak NOE enhancements of H21 with 12α,*β* and H27 with 12α,*β* are only consistent with the two syn orthogonal conformers **3a** and **3c**. The very weak enhancement between the 23-CH_2OH methylene protons and 12α,*β* is only consistent with the predicted syn orthogonal/extended conformer **3g**.

As for the extended conformers, **3b** and **3d**, the strong NOE enhancements of 12α,*β* and H14 upon irradiation of H20 would be consistent with their presence. However, these strong NOE enhancements could reasonably result from an averaged contribution of the syn orthogonal conformers **3a** and **3c**, the anti orthogonal conformers **3e** and **3f**, and the syn orthogonal/extended conformer **3g**. Thus, other reasonable interpretations of the NOE data are feasible. The remaining extended conformer, **3h**, cannot be ruled out with NOE data, but the expected strong enhancement of 16α,*β* upon irradiation of the methylene protons of the 23-CH_2OH group suggests only a minor contribution.

Discussion

The NOE data indicate that **1**−**3** each exist in solution as an equilibrating mixture of conformers. Unlike **3**, both **1** and **2** show the dihedral C18−C17−C20−C21 restricted to a similar range of rotation. For **1** and **2**, the position of the 17α side chain ranged from the syn orthogonal conformers **1a** and **2a** to the anti orthogonal/extended conformers **1c** and **2e**, whereas for **3**, the 17α side chain ranged from the syn orthogonal conformers **3a**/**3c** to the anti orthogonal conformers **3e**/**3f**. In particular, the NOE data indicate that **1d** and **2d**, which are analogous to **3e**/**3f** in side chain position, are not populated. Although the 17α side chain of **1** and **2** appears to have a similar range of rotation, the NOE data do suggest that the relative populations of the major conformers of **1** and **2** are slightly different. For **1**, the NOE data indicates that the major conformer **1c** bears an anti orthogonal/extended 17α side chain, whereas for **2**, the major conformer **2c** has an extended 17α side chain. As for minor conformers, the NOE data suggests that the syn orthogonal conformer **2a** is more abundant in solution for **2** than **1a** is for **1.** This conclusion is rationalized from the H21, 12α,*β* cross-peak found only in the 2D NOESY of **2**.

The presence of the anti orthogonal conformers only found in **3** can be explained by stabilization experienced by **3e** and **3f** as a result of hydrogen bonding between the 17-OH and 23-CH_2OH groups. For **3**, intramolecular hydrogen bonding is not predicted for any of the other conformers according to the MM3 calculations.

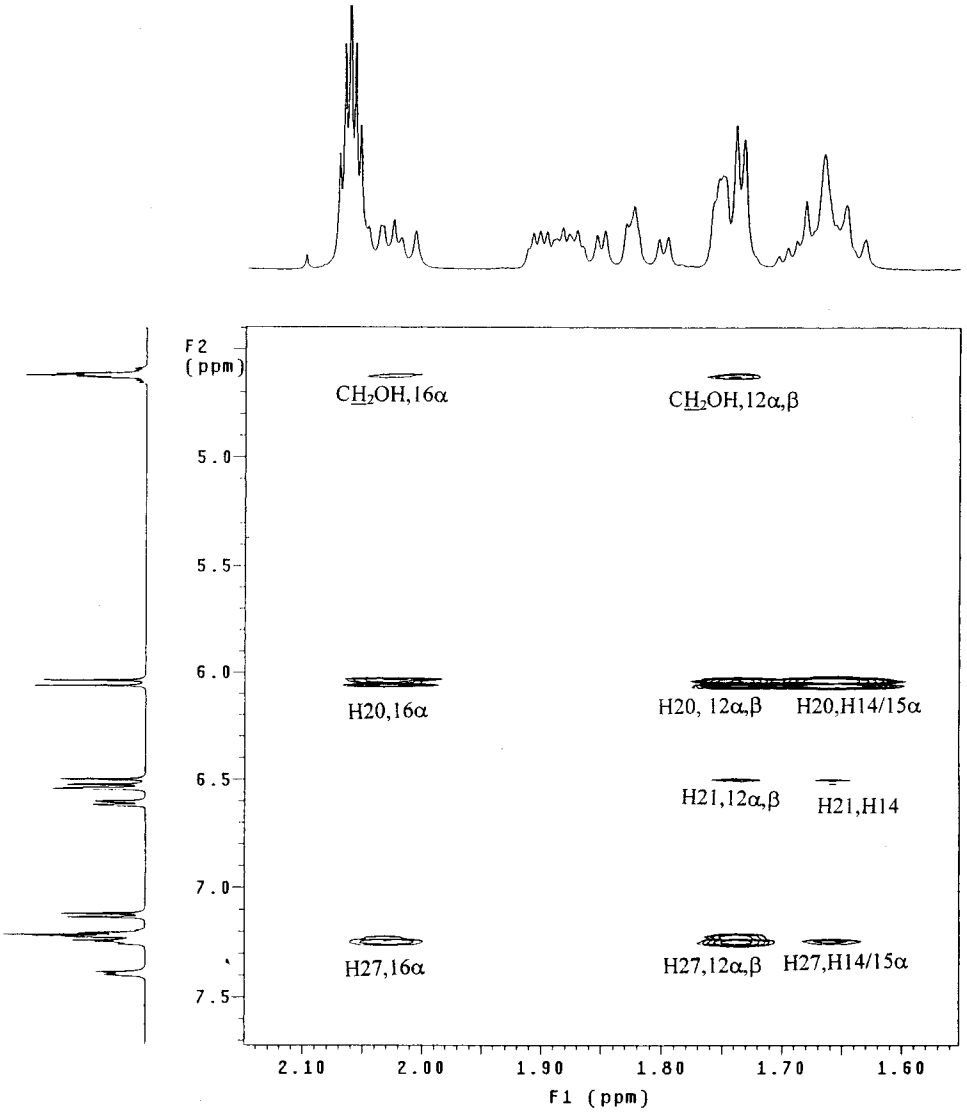

Figure 8. Spectral region of a 500 MHz 2D NOESY spectrum of **3** obtained with a mixing time of 500 ms. The NOE connectivities are indicated.

Table 9. Summary and Comparison of Observed NOE Enhancements with Expected NOE Intensities[a] for Predicted Conformers of 3

irradiated	enhanced	**3a**	**3b**	**3c**	**3d**	**3e**	**3f**	**3g**	**3h**	expt
H20	12α,β	w	s	w	s	s	s	s	s	s
H20	H14	s	s	s	s	w	w	s	s	s
H20	16α	s	w	s	w	w	w	s	w	w
H21	12α,β	w	n	w	n	n	n	n	n	w
H21	H14	n	n	n	n	w	w	n	n	w
H27	12α,β	s	n	s	n	n	n	n	n	w
H27	H14	n	n	n	n	w	w	n	n	w
H27	15α	n	n	n	n	w	w	n	n	w
H27	16α	n	s	n	s	w	w	w	n	w
CH_2OH	12α,β	n	n	n	n	n	n	s	n	w
CH_2OH	16α	w	n	w	n	w	w	n	s	w

[a] Expectations of strong (s), weak (w), and no (n) NOE enhancements correspond to H−H distances of 0−2.99 3.0−4.99, and >5 Å.

The NOE data are mostly consistent with our statistical approach of evaluating contributing conformers from predicted ^{13}C shifts. The findings from multiple independent variable linear regression analysis of the ^{13}C data of **1** and **2**, that the major conformers **1c** and **2c** are 68% and 60% populated and that the minor conformers **1a** and **2a** are both 20% populated, are compatible with the identities of major and minor conformers favored by NOE data. Additionally for **3**, a 36% populated syn orthogonal conformer **3a**, 34% populated extended conformer **3d**, 28% populated anti orthogonal conformer, and 2% populated syn/extended conformer **3g** is quite consistent with the NOE data.

Consistent with the NOE data, the statistical analysis suggests that conformers **1b**, **1e**, and **2d** are not found in solution. For **1**, although a 12% contribution of conformer **1d** is inconsistent with the NOE data, perhaps this is only a minor inconsistency since the identity of the major conformer and another minor conformer are consistent in the two methods. Furthermore, for **2**, a 20% population of conformer **2e** is consistent with the NOE data, although the NOE data do not clearly indicate that **2e** is the only additional minor conformer that is populated.

Conclusions

This study reveals that the substituent on the phenyl group of the 17α,*Z*-phenylvinyl substituent of estradiols can affect the conformational equilibrium of the 17α side chain. Hydrogen bonding stabilization between the 17-

OH and a 23-CH_2OH substituent of **3** results in an additional anti orthogonal conformer not found in **1** or **2**. The similarity in solution conformations of **1** and **2** suggests they occupy a similar receptor volume that is consistent with their similar RBA of 20 and 23 at the estrogen receptor. The different conformational equilibria of **3** may explain its significant RBA of 140, which is greater than estradiol itself. Other effects such as hydrogen bonding, size, and electronic effects of the substituents may also play roles. These results can be applied to the design of subsequent ligands which will examine these conformational and substituent effects.

Experimental Section

HMQC, COSY, 1D and 2D NOESY spectra were obtained on a Varian Unity INOVA instrument at 500 MHz. DEPT and ^{13}C spectra were obtained on a Varian Mercury instrument at 300 MHz.

Acknowledgment. We thank Dr. Roger Kautz for valuable assistance concerning the NMR experiments. This work has been supported in part by PHS award (R01-CA-81049) and a grant from the U.S. Army (DAMD17-99-1-9333).

JO000806H